Inorganica Chimica Acta, *87* (1984) 129–141

Structural Evolution within a Series of Hydrated Bis(dithiooxalato)nickelate(II) of Rare Earths $(RE)_2(H_2O)_{2n}Ni_3(S_2C_2O_2)_6$, xH_2O

J. C. TROMBE, A. GLEIZES and J. GALY

Laboratoire de Chimie de Coordination du C.N.R.S., Associé à l'Université P. Sabatier, 205, route de Narbonne, 31400 Toulouse, France

Received December 14, 1983

Single crystals of a series of hydrated bis(dithiooxalato)nickelate(II) of rare-earths have been synthesized, namely $RE^{(III)}$, Y, La, Ce, Nd, Sm, Eu, Gd, Dy, Er and Yb. The crystal structures were determined by X-ray techniques. The former part of the series (up to Dy) crystallizes in the monoclinic system, space group $P2_1/c$, while the latter part crystallizes in the triclinic system, space group $P\bar{1}$. Full-matrix least-squares refinement led to a final reliability factor $R = 0.0350$ for the europium complex and $R = 0.0266$ for ytterbium.

The characteristic feature of both structures consists of neutral centrosymmetric heteropentanuclear entities $(RE)_2(H_2O)_{2n}Ni_3(S_2C_2O_2)_6$, which only differ by the number n of water-molecules coordinated to the rare earth: $n = 5$ for Eu, while $n = 4$ for Yb. The rare earth atom is also bound to four oxygen atoms of two dithiooxalate groups, so the environment of the europium atom can be represented as a tricapped trigonal prism, while only a bicapped trigonal prism is observed for Yb. The conversion between the two structures involves the loss of one water molecule, in the rare earth sphere of coordination, and a concomitant rearrangement of the ligand dithiooxalate on the summits of the coordination polyhedra.

In both structures the nickel atoms are coordinated to two dithiooxalate groups via *their sulfur atoms.*

The monoclinic network exhibits channels, running parallel to the direction [1 0 0], in which some water molecules are inserted. The triclinic structure can be described as a pseudo lamellar structure, water molecules being inserted between the layers.

Introduction

The anisotropic character of various metallic complexes of the bis(dithiooxalato)nickelate(II) anion has been recently emphasized. Two main kinds of geometries were observed: the first one consists in columnar stacking of nearly planar complex ions, $Ni(S_2C_2O_2)^{2-}$, *e.g.* alkali derivatives [1]; the second one is characterized by extended ordered bimetallic chains, such as for example zinc or manganese derivatives [2, 3].

The synthesis of a series of rare-earth (RE) hydrated bis(dithiooxalato)nickelate(II) has been recently described, with RE(III) = Y, La, Ce, Nd, Sm, Eu, Gd, Dy, Er, Yb [4]. Two kinds of structure were observed: a monoclinic form, space-group $P2_1/c$, from La to Dy included and a triclinic form for the less bulky rare earths, *i.e.* Er and Yb (Table I). Preliminary results concerning the monoclinic structure have already been presented for the europium compound [4]. This preliminary study exhibited the existence of neutral centrosymmetric heteropentanuclear entities $Eu_2(H_2O)_{10}Ni_3(S_2C_2O_2)_6$ called hpe.

From the data reported on Table I, some observations can be drawn:

– within the monoclinic series a decrease of both the *a* and *c* unit-cell constants was noticed,

– the volume of the triclinic form was approximatively half that of the monoclinic form. Assuming that both structures are constituted by hpe, $(RE)_2(H_2O)_{2n}Ni_3(S_2C_2O_2)_6$, the volume difference combined with the experimental specific weight (Table I) was consistent with $Z = 2$ formula per monoclinic unit-cell and only one in the triclinic cell. Moreover a variable amount of inclusion water, xH_2O (Table I) was present in both structures: indeed, the presence of water was ascertained by infrared spectrometry as a broad peak centered at about 3550 cm^{-1}.

In order to confirm these differences and to understand the evolution between the monoclinic and the triclinic forms, the respective structures of the europium and ytterbium compounds (taken as being representative of the two forms) have been determined and are reported in the present paper.

Collection of X-ray Data

The crystal systems and space-groups were determined from single-crystal X-ray photographs obtained by using a precession camera (MoKα).

0020-1693/84/$3.00

TABLE I. Physical and Crystallographic Data of $(RE)_2(H_2O)_{2n}Ni_3(S_2C_2O_2)_6$, xH_2O.

T.R. (III)	La	Ce	Nd	Sm	Eu	Gd	Y	Dy	Er	Yb
r (Å) [5]	1.061	1.034	0.995	0.964	0.950	0.938	0.93	0.908	0.881	0.858
Crystalline system	Monoclinic								Triclinic	
Space group	$P2_1/c$								$P\bar{1}$	
a (Å)	10.451(4)	10.436(9)	10.454(4)	10.459(5)	10.463(2)	10.44(2)	10.44(1)	10.445(1)	10.57(1)	10.572(5)
b (Å)	11.472(9)	11.425(8)	11.428(4)	11.397(6)	11.398(1)	11.358(8)	11.310(6)	11.30(1)	11.094(8)	11.062(3)
c (Å)	20.903(9)	20.84(2)	20.783(9)	20.69(1)	20.703(2)	20.64(3)	20.589(7)	20.56(2)	11.262(9)	11.271(9)
α (°)									108.12(9)	108.02(2)
β (°)	98.89(2)	98.86(4)	99.10(2)	99.18(2)	99.23(1)	99.40(8)	99.62(2)	99.31(1)	91.5(2)	91.97(4)
γ (°)									113.06(7)	112.94(4)
V (Å^3)	2476(2)	2455(3)	2452(2)	2435(2)	2437(2)	2415(6)	2398(2)	2395(6)	1138(7)	1136(2)
Obs. specific weight g/cm^3 ± 0.02	2.08	2.11	2.11	2.17	2.16	2.20	2.02	2.20	2.26	2.28
Inclusion water x(± 1)	11	11.5	10.5	11.5	11.5	11.5	11.5	10.5	9.5	10.

Accurate unit-cell constants (Table I) were refined by optimizing the settling angles of 25 reflections of these single crystals once mounted on a CAD4 ENRAF-NONIUS computer-controlled X-ray diffractometer. The intensity data were collected following the conditions described on Table II.

For the europium compound, 5611 reflections were measured and 3677 independent reflections, with $F_0^2 > 3\sigma(F_0^2)$, were used to refine the structure; these values were respectively 4250 and 3351 for the ytterbium compound. Absorption corrections were performed only for the europium derivative.

Structure Determination and Refinement

The structures were determined by using Patterson and Fourier map techniques, and refined by applying full-matrix least-squares techniques. Throughout the refinement the function minimized was $\Sigma w(F_0 - |F_c|)^2$, where F_0 and F_c are the observed and calculated structure factor amplitudes, and the chosen weighting scheme $w = 4F_0^2/\sigma^2(F_0^2)$.

The atomic scattering factors and their corresponding anomalous terms are those given by Cromer and Waber [6].

The typical unit (hpe) of the monoclinic structure presenting a symmetry center, the space group $P\bar{1}$ was assumed for the triclinic form. The rare-earth and nickel atoms were localized from the Patterson maps: the nickel atom, Ni(2), was placed on a center of inversion. The refinement of the rare-earth and nickel atoms positions, and of the scale factor led to $R = 0.37$ (Eu compound) and $R = 0.33$ (Yb compound). All other non-hydrogen atoms appeared on subsequent Fourier maps. In both structures two kinds of water molecules were observed: water molecules bonded to the rare-earth, and inserted water molecules. Some molecules of the latter kind appeared to be present in non-stoichiometric amounts in the case of the monoclinic structure (Table III). Hydrogen atoms were localized only for water molecules bonded to the rare-earth; their positions were introduced as constants in the refinement. Anisotropic thermal coefficients were used for all the non-hydrogen atoms except for oxygen of inserted water molecules, which were refined isotropically.

The final values of the reliability factors are indicated in Table II; the errors in an observation of unit weight were 2.208 (Eu compound) and 1.817 (Yb compound) electrons. A final difference Fourier map did not show peaks higher than 1/4 (Eu compound) and 1/2 (Yb compound) of the peaks corresponding to a carbon atom in a Fourier map. These residual peaks might be attributed to included water with a very low site occupancy (monoclinic structure) and/or to the rare earth element anisotropy (triclinic structure).

Refined atomic parameters are listed in Table III, and selected interatomic distances and angles in

TABLE II. Experimental Crystallographic Data.

	Eu compound		Yb compound
1) Physical and Crystallographic Data			
Morphology	Elongated parallelepiped (0.043 × 0.015 × 0.013) cm		Elongated parallelepiped (0.023 × 0.008 × 0.005) cm
Abs. factor μ	42.60 cm^{-1}		58.93 cm^{-1}
Transmission factor	0.506–0.671		
2) Data Collection			
Temperature		293 K	
Radiation		$\lambda(MoK\alpha) = 0.71069$	
Crystal detector distance		208 mm	
Detector window			
height		4 mm	
width		4 mm	
Take-off angle	3.75		2.25
Scan-mode	$\theta-2\theta$		ω-scan
Maximum bragg angle	26.5		25
Scan angle			
$\Delta\theta = \Delta\theta_0 + B tg\theta$	$\Delta\theta_0^* = 0.90$		$\Delta\theta_0 = 0.60$
		$B = 0.347$	
Values determining scan speed			
SIGPRE[a]	0.300		0.750
SIGMA[a]	0.018		0.018
VPRE[a]	10°/min		6.7°/min
TMAX[a]	80 sec		80 sec
Controls			
Intensity reflections	$14\bar{3}, 3\bar{1}\bar{1}, 006$		$2\bar{1}4, 02\bar{1}, 100$
periodicity	every 3600 sec		every 3600 sec
Orientation reflections	060, 450, 315		$404, 044, 3\bar{7}0$
periodicity	every 100 reflections		every 100 reflections
3) Conditions for Refinement			
Recorded reflections	5611		4250
Independent reflections			
$I > 3\sigma(I)$	3677		3351
Refined parameters	261		243
Reliability factors			
$R: \Sigma\lvert kF_o - \lvert F_c\rvert\rvert/\Sigma kF_o$	0.0350		0.0266
$R_w = [\Sigma w(kF_o - \lvert F_c\rvert)^2/\Sigma wk^2F_o^2]^{1/2}$	0.0537		0.0327
$w = 4F_o^2/\sigma^2(F_o)^2$			

[a] These parameters have been described in A. Mosset, J. J. Bonnet and J. Galy, *Acta Cryst.*, *B33*, 2633 (1977).

Table IV. A listing of observed and calculated structure amplitudes is available as supplementary material.

Description of the Structures

The main similarity between the structures consists in the existence of a neutral centrosymmetric heteropentanuclear entity (hpe), $(RE)_2(H_2O)_{2n}Ni_3(S_2C_2O_2)_6$, which constitutes the basic unit of the structures. The existence of such hpe appears to obey the electroneutrality rule. It is noticeable that rare-earth complexes of the bis(dithiooxalato)nickelate(II) anion behave as an intermediary between alkali derivatives, in which isolated $Ni(S_2C_2O_2)_2^{2-}$ ion occur [1] with 'infinite' chains represented by the manganese derivative [3]. However, whatever their similarities, the two hpe exhibit differences relative to their composition, geometry and stacking.

A projection of the hpe onto the (100) plane is presented in Fig. 1. In both cases, the hpe develops mainly along the *c* axis: however they are tilted with respect to the (100) plane by a mean angle of 27°6 (Eu) and 25°2 (Yb). They are quite comparable, allowing only for some small changes of length due to the shortening of the rare-earth radius. So the distances RE–Ni(1) and RE–Ni(2) are respectively

TABLE III. Positional and Thermal Parameters for the Atoms of $(RE)_2(H_2O)_{2n}Ni_3(S_2C_2O_2)_6$, xH_2O.[a]

Atom	x	y	z	B_{11} B_{22} B_{33}	B_{12} B_{13} B_{23}
Eu	0.07994(3)	−0.04187(3)	0.30365(1)	2.83(2) 1.79(1) 1.53(1)	0.11(1) 0.259(9) −0.253(9)
Ni(1)	0.32869(8)	−0.42241(8)	0.49900(4)	2.90(4) 2.02(4) 1.93(3)	0.21(3) 0.02(3) 0.31(3)
Ni(2)	0	0	0	2.82(5) 1.94(4) 1.45(4)	−0.22(4) 0.38(3) 0.06(3)
S_{11}	0.3601(2)	−0.6117(2)	0.49819(9)	3.80(8) 2.41(7) 2.66(7)	0.42(6) 0.62(6) 0.06(5)
S_{12}	0.3639(2)	−0.4180(2)	0.60535(8)	3.90(8) 2.53(7) 2.14(6)	0.28(6) −0.00(6) 0.24(5)
S_{21}	0.2736(2)	−0.4237(1)	0.39196(8)	3.14(7) 2.02(6) 2.11(6)	0.49(5) 0.04(5) 0.01(5)
S_{22}	0.3034(2)	−0.2334(2)	0.50331(8)	5.4(1) 2.27(7) 1.96(6)	0.27(7) 0.63(6) −0.04(5)
S_{31}	−0.0025(2)	−0.1461(2)	0.06792(8)	4.51(9) 2.00(7) 1.86(6)	−0.63(6) 0.33(6) 0.02(5)
S_{32}	0.0641(2)	0.1233(1)	0.07869(7)	3.19(7) 1.94(6) 1.68(6)	−0.29(5) 0.53(5) 0.16(5)
O_{11}	0.4251(7)	−0.7520(5)	0.5972(3)	7.6(4) 3.1(3) 4.3(3)	1.1(3) 2.2(3) 1.0(2)
O_{12}	0.4029(6)	−0.5910(6)	0.6874(3)	6.1(3) 4.0(3) 2.9(2)	1.9(2) 0.8(2) 1.0(2)
O_{21}	0.1602(4)	−0.2522(4)	0.3198(2)	2.8(2) 2.0(2) 1.9(2)	0.1(2) −0.1(1) 0.2(1)
O_{22}	0.2241(6)	−0.0890(5)	0.4078(2)	6.0(3) 1.9(2) 2.5(2)	0.0(2) −0.7(2) 0.3(2)
O_{31}	0.0349(6)	−0.1398(4)	0.1953(2)	5.3(3) 2.3(2) 2.1(2)	−0.5(2) 0.8(2) 0.2(2)
O_{32}	0.0911(5)	0.0858(4)	0.2046(2)	2.6(2) 2.3(2) 1.8(2)	0.5(2) 0.5(2) 0.2(2)
C_{11}	0.3963(7)	−0.6537(6)	0.5788(4)	3.4(3) 2.2(3) 3.6(3)	0.6(2) 1.5(3) 1.1(2)
C_{12}	0.3902(7)	−0.5597(6)	0.6306(3)	2.9(3) 2.5(3) 2.3(3)	0.6(2) 0.4(2) −0.3(2)

(continued on facing page)

TABLE III *(continued)*

Atom	*x*	*y*	*z*	B_{11} B_{22} B_{33}	B_{12} B_{13} B_{23}
C_{21}	0.2201(6)	−0.2851(6)	0.3739(3)	2.2(3) 2.0(3) 1.9(2)	0.0(2) 0.3(2) 0.0(2)
C_{22}	0.2469(6)	−0.1919(6)	0.4253(3)	2.6(3) 2.1(3) 2.2(3)	0.0(2) −0.2(2) 0.2(2)
C_{31}	0.0331(6)	−0.0848(6)	0.1424(3)	2.4(3) 2.5(3) 1.9(3)	0.0(2) 0.2(2) 0.0(2)
C_{32}	0.0642(6)	−0.0438(6)	0.1474(3)	1.8(2) 2.5(3) 1.6(2)	−0.1(2) 0.2(2) 0.2(2)
Ow(1)	−0.1054(5)	−0.1664(5)	0.3026(3)	3.4(2) 2.2(2) 5.4(3)	−0.3(2) 0.5(2) −0.5(2)
Ow(2)	−0.1103(5)	0.0777(5)	0.2744(3)	4.2(3) 2.8(2) 3.6(2)	1.0(2) 1.3(2) −1.5(2)
Ow(3)	0.2955(5)	−0.0456(5)	0.2779(3)	3.4(2) 4.6(3) 4.4(3)	0.8(2) 1.4(2) 1.1(2)
Ow(4)	0.1604(6)	0.1472(5)	0.3411(3)	5.5(3) 2.7(2) 4.1(3)	−0.5(2) 0.9(2) −0.9(2)
Ow(5)	−0.0180(7)	0.0076(8)	0.4021(3)	6.0(4) 9.7(5) 2.5(3)	−2.0(4) 1.7(2) −0.5(3)
Ow(6)	−0.1665(7)	−0.0951(8)	0.4871(4)	6.4(2)	
Ow(7)	0.4404(8)	−0.2335(8)	0.2543(4)	7.1(2)	
0.5Ow(8)	−0.313(1)	0.116(1)	0.3425(6)	4.5(2)	
0.5Ow(9)	−0.342(2)	−0.113(2)	0.2340(9)	8.0(4)	
0.5Ow(10)	0.441(2)	−0.959(2)	0.526(1)	8.8(5)	
0.5Ow(11)	0.409(2)	0.168(2)	0.388(1)	9.6(5)	
0.5Ow(12)	0.479(2)	−0.989(2)	0.600(1)	9.4(5)	
H_1Ow(1)	−0.178	−0.175	0.266	3.5	
H_2Ow(1)	−0.107	−0.250	0.300	3.5	
H_1Ow(2)	−0.107	0.150	0.250	3.4	
H_2Ow(2)	−0.175	0.037	0.288	3.4	
H_1Ow(3)	0.321	−0.100	0.266	4.0	
H_2Ow(3)	0.321	0.025	0.250	4.0	
H_1Ow(4)	0.107	0.200	0.350	4.0	
H_2Ow(4)	0.250	0.150	0.350	4.0	
H_2Ow(5)	0.036	0.025	0.434	5.8	
H_2Ow(5)	−0.071	−0.025	0.427	5.8	
Yb	0.06596(3)	−0.24789(3)	0.39746(2)	2.21(1) 1.29(1) 1.52(1)	0.808(8) 0.065(7) 0.639(7)
Ni(1)	0.33816(8)	0.01982(7)	0.94964(7)	2.41(4) 1.66(4) 1.53(4)	0.79(4) 0.10(3) 0.93(3)
Ni(2)	0	0	0	2.71(3) 1.60(3) 1.59(3)	0.74(3) −0.15(3) 0.64(3)

(continued overleaf

TABLE III *(continued)*

Atom	x	y	z	B_{11} B_{22} B_{33}	B_{12} B_{13} B_{23}
S_{11}	0.3547(2)	−0.0570(2)	1.1028(1)	3.11(7)	0.87(5)
				1.75(6)	0.02(5)
				1.78(6)	0.72(5)
S_{12}	0.4276(2)	0.2351(2)	1.0788(1)	4.21(8)	0.92(6)
				1.62(6)	−0.28(6)
				2.02(7)	0.70(5)
S_{21}	0.2436(2)	−0.1975(2)	0.8177(1)	3.34(7)	0.86(5)
				1.65(6)	−0.21(5)
				1.88(6)	0.80(5)
S_{22}	0.3129(2)	0.1011(2)	0.8007(1)	3.73(8)	0.70(5)
				1.50(6)	−0.45(5)
				1.85(6)	0.59(5)
S_{31}	−0.0538(2)	−0.2132(2)	−0.0037(1)	3.32(7)	0.82(5)
				1.72(6)	−0.15(5)
				1.67(6)	0.78(5)
S_{32}	0.0832(2)	0.0914(1)	0.2025(1)	2.95(7)	0.89(5)
				1.58(6)	0.05(5)
				1.76(6)	0.89(5)
O_{11}	0.4341(5)	0.0819(4)	1.3456(4)	4.5(2)	0.8(2)
				2.4(2)	0.2(2)
				1.8(2)	0.9(2)
O_{12}	0.4914(6)	0.3331(5)	1.3250(4)	6.6(3)	1.5(2)
				2.2(2)	0.1(2)
				2.3(2)	0.5(2)
O_{21}	0.1384(4)	−0.2865(4)	0.5772(4)	3.8(2)	1.0(2)
				1.4(2)	−0.4(2)
				2.0(2)	0.5(1)
O_{22}	0.1613(4)	−0.0446(4)	0.5755(4)	3.7(2)	1.4(2)
				2.0(2)	−0.2(2)
				1.7(2)	0.9(1)
O_{31}	−0.0151(5)	−0.2911(4)	0.1862(4)	3.7(2)	1.2(2)
				1.6(2)	0.1(2)
				2.2(2)	1.0(1)
O_{32}	0.1078(4)	−0.0393(4)	0.3522(4)	3.7(2)	0.9(2)
				1.4(2)	0.0(1)
				1.9(2)	0.9(1)
C_{11}	0.4151(6)	0.0863(6)	1.2387(6)	2.2(3)	0.6(2)
				1.6(2)	0.4(2)
				2.3(3)	0.7(2)
C_{12}	0.4498(6)	0.2308(6)	1.2275(6)	3.0(3)	1.0(2)
				2.1(3)	0.2(2)
				2.0(3)	0.8(2)
C_{21}	0.1942(6)	−0.1870(6)	0.6800(5)	2.1(2)	0.9(2)
				1.6(2)	0.3(2)
				1.9(3)	0.7(2)
C_{22}	0.2163(6)	−0.0436(6)	0.6756(5)	2.4(3)	0.9(2)
				1.5(2)	0.5(2)
				1.9(2)	0.7(2)
C_{31}	−0.0024(6)	−0.1936(6)	0.1462(5)	2.2(2)	1.0(2)
				1.9(2)	0.4(2)
				1.8(2)	0.8(2)

(continued on facing page)

TABLE III *(continued)*

Atom	*x*	*y*	*z*	B_{11} B_{22} B_{33}	B_{12} B_{13} B_{23}
C_{32}	0.0676(6)	−0.0469(6)	0.2446(5)	1.9(2) 2.1(2) 1.7(2)	1.0(2) 0.3(2) 1.1(2)
Ow(1)	−0.1161(5)	−0.4484(4)	0.3990(5)	3.0(1) 1.7(2) 4.8(3)	0.9(2) 1.0(2) 1.3(2)
Ow(2)	−0.1261(4)	−0.2070(4)	0.4397(4)	2.4(2) 1.5(2) 4.4(2)	0.9(2) 0.4(2) 0.5(2)
Ow(3)	0.2932(4)	−0.1648(4)	0.3778(5)	2.7(2) 2.6(2) 5.0(3)	1.3(2) 1.1(2) 2.3(2)
Ow(4)	0.1020(5)	−0.4416(5)	0.2799(4)	4.4(2) 2.4(2) 3.1(2)	2.0(2) 0.8(2) 0.8(2)
Ow(5)	−0.3746(5)	−0.4003(5)	0.2974(4)	3.16(9)	
Ow(6)	0.4488(5)	−0.2962(5)	0.4194(4)	3.34(9)	
Ow(7)	−0.3564(5)	−0.4510(6)	0.0428(5)	4.2(1)	
Ow(8)	0.2486(5)	−0.5522(6)	0.3986(5)	4.6(1)	
Ow(9)	0.1725(7)	−0.4229(7)	0.0498(7)	6.9(2)	
H_1Ow(1)	−0.100	−0.525	0.350	3.1	
H_2Ow(1)	−0.175	−0.450	0.475	3.1	
H_1Ow(2)	−0.200	−0.275	0.400	2.8	
H_2Ow(2)	−0.125	−0.125	0.475	2.8	
H_1Ow(3)	0.325	−0.075	0.375	3.3	
H_2Ow(3)	0.350	−0.200	0.400	3.3	
H_1Ow(4)	0.100	−0.475	0.200	3.1	
H_2Ow(4)	0.125	−0.500	0.300	3.1	

[a] Estimated standard deviations in the last significant figure are given in parentheses. Isotropic *B*'s and anisotropic *Bij*'s thermal parameters have unit of Å^2. Anisotropic parameters enter the expression of the structure factor in the form $\exp[0.25(B_{11}a^{*2}h^2 + B_{22}b^{*2}k^2 + B_{33}c^{*2}l^2 + 2B_{12}a^*b^*hk + 2B_{13}a^*c^*hl + 2B_{23}b^*c^*kl)]$.

6.21 and 6.23 Å in the case of Eu, and 6.04, 6.07 Å in the case of Yb; the observed differences 0.17 and 0.16 Å are greater than the difference of radius between Eu(III) and Yb(III) (Table I). The angles Ni(1)–RE–Ni(2) are comparable: Ni(1)–Eu–Ni(2) = 133.3° and Ni(1)–Yb–Ni(2) = 132°1.

In both structures the central nickel atom Ni(2) is located on a crystallographic inversion center. This nickel atom, as well as Ni(1), is coordinated to four sulfur atoms of two dithiooxalate groups. The distances Ni–S and the angles around the nickel atoms are quite comparable for Ni(1) and Ni(2), and they show no significant difference from one structure to the other (Table IV). In the same way, the differences concerning the S–C, C–O and C–C distances are minor, with the exception of the terminal dithiooxalate groups of the hpe (Fig. 1, Table IV): these latter groups present larger S–C bonds and shorter C–O bonds than the corresponding groups of the middle of the hpe.

The anion $Ni(S_2C_2O_2)^{2-}$ has previously been shown to present only slight deviations from planarity, in the case of alkali derivatives [1]. The equation of least-squares planes and the corresponding atom-to-plane distances have been calculated for different parts of the anion *i.e.*, the plane of coordination of the nickel atom and each 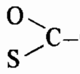 $\overset{O}{\underset{S}{>}}C\text{–}C$ part of the dithiooxalate group. In the Yb compound the dithiooxalate group is slightly less distorted than in the Eu one. Within an hpe (Fig. 1) the deformation of the various dithiooxalate groups seems to be related to their respective location: the more distorted dithiooxalate group is the one linked both to Ni(1) and to the RE atoms (Fig. 1, Table V).

The mean deviations from planarity of the dithiooxalate group in the rare-earths compounds are slightly more important than those observed in alkali or Ba derivatives [1, 7].

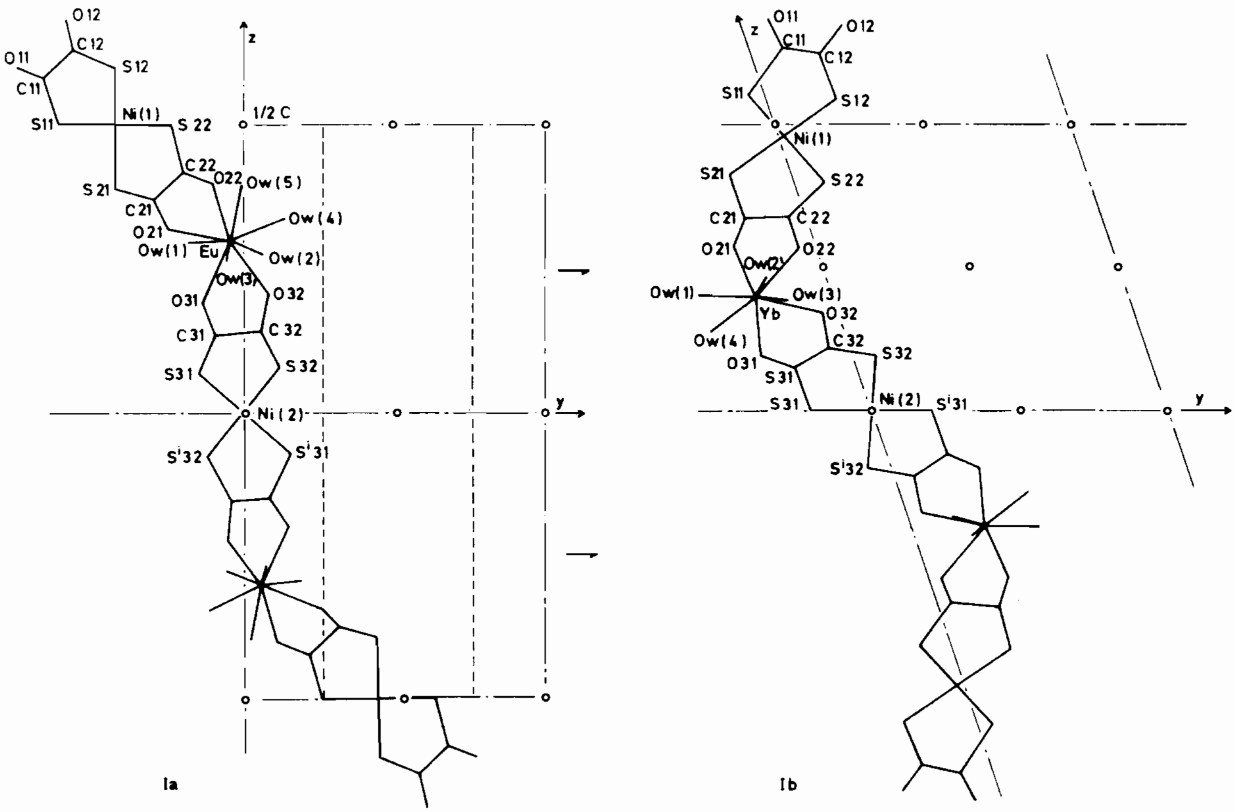

Fig. 1. Projection of the centrosymmetric heteropentanuclear entities on the (100) plane: Ia: monoclinic structure; Ib: triclinic structure.

TABLE IV. Selected Interatomic Distances (Å) and Bonds Angles (deg.).

Around RE	Eu	Yb
RE–$\mathrm{O_{21}}$	2.544(4)	2.359(4)
RE–$\mathrm{O_{22}}$	2.484(5)	2.329(4)
RE–$\mathrm{O_{31}}$	2.482(5)	2.341(4)
RE–$\mathrm{O_{32}}$	2.533(4)	2.395(4)
RE–Ow(1)	2.401(5)	2.311(4)
RE–Ow(2)	2.408(5)	2.281(4)
RE–Ow(3)	2.400(5)	2.262(4)
RE–Ow(4)	2.396(5)	2.326(4)
RE–Ow(5)	2.489(6)	

Around Ni(1)	Eu	Yb
Ni(1)–$\mathrm{S_{11}}$	2.185(2)	2.177(2)
Ni(1)–$\mathrm{S_{12}}$	2.174(2)	2.170(2)
Ni(1)–$\mathrm{S_{21}}$	2.199(2)	2.196(2)
Ni(1)–$\mathrm{S_{22}}$	2.174(2)	2.189(2)
$\mathrm{S_{11}}$–Ni(1)–$\mathrm{S_{22}}$	177.7(1)	176.7(1)
$\mathrm{S_{12}}$–Ni(1)–$\mathrm{S_{21}}$	174.6(1)	178.7(3)
$\mathrm{S_{11}}$–Ni(1)–$\mathrm{S_{12}}$	91.69(7)	91.75(6)
$\mathrm{S_{11}}$–Ni(1)–$\mathrm{S_{21}}$	90.08(7)	88.93(6)
$\mathrm{S_{22}}$–Ni(1)–$\mathrm{S_{12}}$	86.41(7)	86.90(6)
$\mathrm{S_{22}}$–Ni(1)–$\mathrm{S_{21}}$	91.93(7)	92.93(7)
	360.11	360.51

TABLE IV *(continued)*

Around Ni(2)	Eu	Yb
Ni(2)–$\mathrm{S_{31}}$	2.182(2)	2.188(2)
Ni(2)–$\mathrm{S_{32}}$	2.174(2)	2.182(2)
$\mathrm{S_{31}}$–Ni(2)–$\mathrm{S_{32}}$	87.45(6)	92.79(6)
$\mathrm{S_{31}}$–Ni(2)–$\mathrm{S_{32}}^{i}$	92.55(6)	87.25(6)
$\mathrm{S_{31}}$–Ni(2)–$\mathrm{S_{31}}^{i}$	180.	180.

Dithiooxalate ligand	Eu	Yb
$\mathrm{S_{11}}$–$\mathrm{C_{11}}$	1.719(7)	1.709(6)
$\mathrm{S_{12}}$–$\mathrm{C_{12}}$	1.706(7)	1.703(6)
$\mathrm{S_{21}}$–$\mathrm{C_{21}}$	1.697(6)	1.674(6)
$\mathrm{S_{22}}$–$\mathrm{C_{22}}$	1.697(6)	1.684(6)
$\mathrm{O_{11}}$–$\mathrm{C_{11}}$	1.206(9)	1.234(7)
$\mathrm{O_{12}}$–$\mathrm{C_{12}}$	1.216(8)	1.223(7)
$\mathrm{O_{21}}$–$\mathrm{C_{21}}$	1.250(7)	1.251(7)
$\mathrm{O_{22}}$–$\mathrm{C_{22}}$	1.239(8)	1.248(7)
$\mathrm{C_{11}}$–$\mathrm{C_{12}}$	1.498(9)	1.542(7)
$\mathrm{C_{21}}$–$\mathrm{C_{22}}$	1.524(1)	1.528(7)
Ni(1)–$\mathrm{S_{11}}$–$\mathrm{C_{11}}$	103.1(3)	106.0(2)
Ni(1)–$\mathrm{S_{12}}$–$\mathrm{C_{12}}$	106.3(3)	106.9(2)
Ni(1)–$\mathrm{S_{21}}$–$\mathrm{C_{21}}$	103.9(2)	104.7(2)
Ni(1)–$\mathrm{S_{22}}$–$\mathrm{C_{22}}$	105.3(2)	103.9(2)

(continued on facing page)

TABLE IV *(continued)*

Dithiooxalate	Eu	Yb
$S_{11}{-}C_{11}{-}C_{12}$	117.4(5)	118.1(4)
$S_{11}{-}C_{11}{-}O_{11}$	124.8(6)	124.1(4)
$O_{11}{-}C_{11}{-}C_{12}$	117.9(7)	117.7(5)
	360.1	359.9
$S_{31}{-}C_{31}$	1.680(6)	1.679(6)
$S_{32}{-}C_{32}$	1.686(6)	1.690(5)
$O_{31}{-}C_{31}$	1.259(8)	1.256(7)
$O_{32}{-}C_{32}$	1.267(7)	1.238(6)
$C_{31}{-}C_{32}$	1.501(9)	1.521(8)
$S_{31}{-}S_{32}$	3.011(2)	3.013(2)
$S_{31}{-}S_{32}i$	3.148(2)	3.164(2)
$S_{31}{-}O_{31}$	2.604(5)	2.617(4)
$S_{32}{-}O_{32}$	2.611(4)	2.604(4)
$O_{31}{-}O_{32}$	2.638(7)	2.600(6)
$S_{11}{-}S_{12}$	3.125(3)	3.120(2)
$S_{11}{-}S_{21}$	3.100(3)	3.063(2)
$S_{12}{-}S_{22}$	2.977(3)	2.998(2)
$S_{21}{-}S_{22}$	3.144(2)	3.164(2)
$S_{11}{-}O_{11}$	2.603(6)	2.610(4)
$S_{12}{-}O_{12}$	2.592(6)	2.605(5)
$S_{21}{-}O_{21}$	2.625(5)	2.619(4)
$S_{22}{-}O_{22}$	2.604(5)	2.610(4)
$O_{11}{-}O_{12}$	2.655(9)	2.693(6)
$O_{21}{-}O_{22}$	2.615(7)	2.599(5)
$S_{12}{-}C_{12}{-}C_{11}$	118.2(5)	116.9(4)
$S_{12}{-}C_{12}{-}O_{12}$	124.1(6)	125.0(4)
$O_{12}{-}C_{12}{-}C_{11}$	117.6(6)	118.1(1)
	359.9	360.0
$S_{21}{-}C_{21}{-}C_{22}$	119.0(4)	118.6(4)
$S_{22}{-}C_{22}{-}O_{22}$	125.3(5)	126.5(4)
$O_{21}{-}C_{21}{-}C_{22}$	115.6(6)	114.9(5)
	359.9	360.0
$S_{22}{-}C_{22}{-}C_{21}$	118.4(5)	119.3(4)
$S_{22}{\leftrightarrow}\underline{\,\vert\,}_{2}{-}O_{22}$	124.2(5)	125.1(4)
$O_{22}{-}C_{22}{-}C_{21}$	117.4(6)	115.6(5)
	360.0	360.0
$Ni(2){-}S_{31}{-}C_{31}$	104.5(2)	104.5(2)
$Ni(2){-}S_{32}{-}C_{32}$	104.1(2)	104.3(2)
$S_{31}{-}C_{31}{-}C_{32}$	118.8(5)	119.1(4)
$S_{31}{-}C_{31}{-}O_{31}$	124.2(5)	125.6(4)
$O_{31}{-}C_{31}{-}C_{32}$	117.0(5)	115.3(5)
	360.0	360.0
$S_{32}{-}C_{32}{-}C_{31}$	119.8(4)	119.2(4)
$S_{32}{-}C_{32}{-}O_{32}$	123.7(5)	124.8(4)
$O_{32}{-}C_{32}{-}C_{31}$	116.5(5)	116.0(5)
	360.0	360.0

TABLE IV *(continued)*

Van der Waals contacts

	Eu		Yb
Ow(10)–O_{11}	2.80(2)	Ow(3)–O_{11}^{ii}	2.700(6)
Ow(12)–O_{11}	2.76(2)	Ow(6)–O_{11}^{iii}	2.792(6)
Ow(3)–O_{12}^{iv}	2.806(8)	Ow(2)–Ow(1)	2.612(6)
Ow(7)–O_{12}^{v}	2.74(1)	Ow(2)–Ow(5)	2.701(6)
Ow(2)–O_{21}^{ii}	2.740(6)	Ow(4)–Ow(1)	2.694(7)
Ow(5)–O_{22}	2.75(1)	Ow(4)–Ow(3)	2.765(6)
Ow(2)–O_{32}	2.741(7)	Ow(4)–Ow(9)	2.770(9)
Ow(1)–Ow(9)	2.72(2)	Ow(1)–Ow(8)^{iv}	2.716(7)
Ow(2)–Ow(8)	2.76(1)	Ow(3)–Ow(6)	2.697(6)
Ow(2)–Ow(5)	2.783(8)	Ow(5)–Ow(6)^{v}	2.751(7)
Ow(3)–Ow(7)	2.71(1)	Ow(5)–Ow(7)	2.779(7)
Ow(4)–Ow(11)	2.64(2)	Ow(6)–Ow(8)^{vi}	2.732(7)
Ow(5)–Ow(6)	2.79(1)		
Ow(7)–Ow(9)^{vi}	2.75(2)		
Ow(8)–Ow(12)^{vii}	2.76(1)		

Nickel–Nickel distances

	Eu		Yb
Ni(1)–Ni(2)^{viii}	3.554(1)	Ni(1)–Ni(2)^{vii}	3.573(2)
Ni(1)–Ni(1)^{v}	3.992(2)	Ni(1)–Ni(1)^{viii}	3.797(2)

Code of equivalent positions relative to x, y, z

Eu				Yb			
i:	$\bar{x}$	$\bar{y}$	$\bar{z}$	i:	$\bar{x}$	$\bar{y}$	$\bar{z}$
ii:	$\bar{x}$	1/2 + y	1/2 − z	ii:	x	y	$\bar{1}$ + z
iii:	x	1/2 − y	1/2 + z	iii:	1 − x	$\bar{y}$	$\bar{2}$ − z
iv:	x	$\bar{1}/\bar{2}$ − y	$\bar{1}/\bar{2}$ + z	iv:	$\bar{x}$	$\bar{1}$ − y	1 − z
v:	1 − x	$\bar{1}$ − y	1 − z	v:	$\bar{1}$ + x	y	z
vi:	1 + x	y	z	vi:	$\bar{x}$	1 − y	$\bar{z}$
vii:	$\bar{x}$	$\bar{1}$ − y	1 − z	vii:	x	y	1 + z
viii:	1 − x	$\bar{y}$	2 − z	viii:	1 − x	$\bar{y}$	2 − z

The RE atom is linked to two dithiooxalate groups through their oxygen atoms (Fig. 1). The rare-earth coordination is completed by five water molecules for the monoclinic structure and only four water molecules for the triclinic structure. The Eu coordination polyhedron is a distorted tricapped trigonal prism while the Yb one is a distorted bicapped trigonal prism (Fig. 2). As expected the Yb–O bond lengths are significantly shorter than the Eu–O ones (Table IV).

However, the mean shortening, 0.15 Å for oxygen atoms from dithiooxalate groups and 0.12 Å for oxygen atoms from water molecules, is larger than the difference of radius of the two RE, 0.09 Å (Table I). Besides, the distances RE–oxygen of water molecules are generally shorter than the distances RE–oxygen of dithiooxalate groups: the only exception corresponds to the water molecule Ow(5) of

TABLE V. Least-squares Planes, Atom to Plane Distances (10^{-3} Å) and Dihedral Angles in the Anion $Ni(S_2C_2O_2)^{2-}$, for the Eu and Yb Compounds.

Plane I	Eu	Yb	Plane II	Eu	Yb	Plane III	Eu	Yb
Ni(1)	19	18	Ni(2)	0	0	S_{11}	0	0
S_{11}	40	−38	S_{31}	0	0	O_{11}	−1	1
S_{12}	−87	−1	S_{32}	0	0	C_{11}	4	−5
S_{21}	−72	−2				C_{12}	−1	1
S_{22}	45	−4						
Plane IV	**Eu**	**Yb**	**Plane V**	**Eu**	**Yb**	**Plane VI**	**Eu**	**Yb**
S_{12}	0	0	S_{21}	0	0	S_{22}	0	0
O_{12}	2	0	O_{21}	1	−1	O_{22}	−2	2
C_{11}	2	0	C_{21}	−6	4	C_{21}	−2	2
C_{12}	−5	−2	C_{22}	2	1	C_{22}	7	−8
Plane VII	**Eu**	**Yb**	**Plane VIII**	**Eu**	**Yb**			
S_{31}	0	0	S_{32}	0	0			
O_{31}	1	1	O_{32}	−1	−1			
C_{31}	−2	−4	C_{31}	−2	−2			
C_{32}	1	1	C_{32}	6	6			
Plane IX	**Eu**	**Yb**	**Plane X**	**Eu**	**Yb**	**Plane XI**	**Eu**	**Yb**
Ni(1)	−2	−9	Ni(1)	−18	−14	Ni(2)	0	0
S_{11}	−3	31	S_{21}	83	30	S_{31}	45	−8
S_{12}	19	38	S_{22}	42	76	S_{32}	40	−20
O_{11}	100	−70	O_{21}	−313	54	O_{31}	−108	−20
O_{12}	−149	−120	O_{22}	89	−289	O_{32}	−109	82
C_{11}	33	−41	C_{21}	97	5	C_{31}	−41	−6
C_{12}	−39	−52	C_{22}	27	−99	C_{32}	−50	32

Dihedral angles		I–III	I–IV	1–V	I–VI
Eu		5.25	8.26	15.34	7.72
Yb		5.27	6.59	6.07	13.51
		II–VII	II–VIII	III–IV	III–V
Eu		5	4.95	6.51	17.86
Yb		1.44	3.23	1.36	9.72
	III–VI	IV–V	IV–VI	V–VI	VII–VIII
Eu	12.59	23.36	15.64	10.78	0.19
Yb	18.43	11.01	19.79	9.45	2.85

the europium compound (Table IV), its distance from Eu being comparable to some Eu–O distances from dithiooxalate groups. The RE–oxygen distances can also be related to the respective location of the oxygen atom on the coordination polyhedron, the ones on summits of the trigonal prism (*e.g.* O_{31}, Ow(1)...) being closer to the rare earth atom than those located at the capping positions (Table IV, Fig. 1).

The stacking of the Ni dithiooxalate groups (Fig. 3) is similar in both structures, but it differs markedly from the modes of stacking encountered in the alkali and alkaline-earths salts, and also in the manganese complex [1, 3, 7]. One single stack is made of sequences of three $Ni(S_2C_2O_2)_2^{2-}$ groups, repeating along the [1 0 0] direction. A sequence includes a Ni(2) atom located at a center of inversion and two Ni(1) atoms related through this center (Fig. 3). In

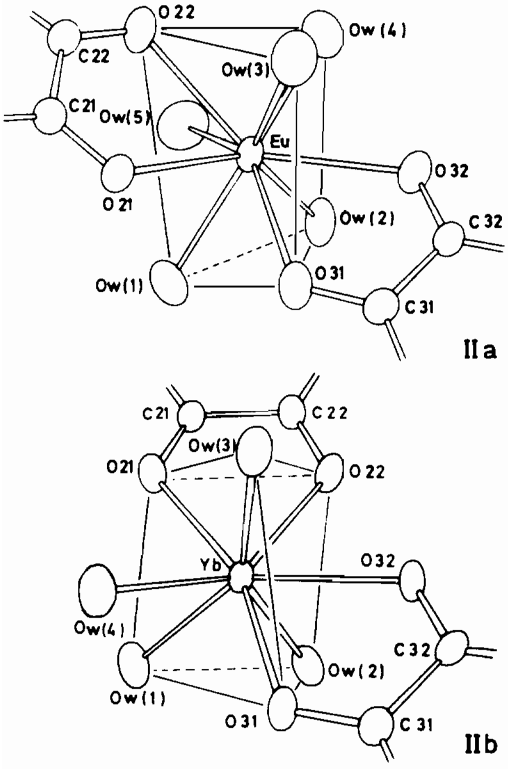

Fig. 2. The polyhedron of coordination of the rare earth: IIa: monoclinic structure; IIb: triclinic structure.

such a sequence two successive NiS_4 groups are staggered by about 45° around the normal to their quite parallel mean planes; however the Ni(1)–Ni(2)–Ni(1)^i direction makes an angle of 4.43° (Eu compound) and of 3.93° (Yb compound) with this normal. Two successive sequences of three $Ni(S_2C_2O_2)_2{}^{2-}$ groups are related by the a translation, so that the top group of one sequence partially eclipses the bottom group of the next one. Consequently the Ni–Ni spacings within a sequence 3.554(1) Å (Eu compound) and 3.573(2) Å (Yb compound) are significantly shorter than the closest Ni–Ni distances between two sequences, 3.992(2) Å (Eu compound) and 3.797(2) Å (Yb compound). The distances between NiS_4 mean planes, within a sequence, are roughly the same, *i.e.* 3.54 Å (Eu compound) and 3.56 Å (Yb compound). This kind of stacking of the $Ni(S_2C_2O_2)_2{}^{2-}$ groups is directly related with the weak conductivity observed for these bis(dithiooxalato)nickelate(II) of rare-earths [4].

The hpe stacking for both structures is presented in Fig. 4. In both cases the lattice cohesion occurs by inter-hpe links, through hydrogen bonds (Table IV) arising between oxygen atoms either from dithiooxalate groups or from water molecules bonded or not to the rare earth. The shortest distances between hpe involves particularly the oxygen atoms of the terminal dithiooxalate groups on the hpe, and water molecules. These distances are approximately twice the Van der Waals radius of oxygen atom [8].

The monoclinic compounds can be considered as a channel structure, the water molecules being inserted within the channels (Fig. 4). Some of the possible crystallographic sites are only statistically occupied (Table III), and it is likely that additional water molecules with a low site occupancy are present in the lattice. In fact the experimental specific weight is somewhat greater than the calculated one, and residual peaks on the last Fourier difference map can be attributed to such molecules. Furthermore the europium bis(dithiooxalato)nickelate(II) crystals appear to be very sensitive to dryness.

As regard to the triclinic compounds, they can be described as a pseudolamellar structure, a bed of water molecules occupying the interlayers spaces (Fig. 4). The number of water molecules deduced from the experimental density and observed by X-ray diffraction is quite similar (Table I and III).

A Preliminary Proposal for the Evolution between the Two Structures

An interpretation of the modification of CN number of the rare-earth, between the two structures, can be proposed on the basis of the observed distances RE–oxygen, oxygen–oxygen, and of the distribution of oxygen atoms around the rare earth.

As shown in Table VI, some oxygen atoms (either from dithiooxalate groups or from water) are in close contact or are very near, relative to the europium compound: this is particularly the case for the water molecule Ow(5) with Ow(2) or O_{22} (Table VI).

When the RE radius is decreasing (Table I), the distances RE oxygen will also decrease. Assuming that the geometry of coordination is not greatly affected within the monoclinic series, the shortening of the distances will tend to bring nearer the trigonal bases of the prism. The atoms located on the capping positions must also shift towards the rare-earth atom, but such a possibility is very limited for these atoms, particularly for Ow(5) which is already very squeezed in the europium structure. As the RE radius is decreasing, the Ow(5) molecule will become less and less bound to the rare-earth atom, up to a certain limit where there will be no more interaction. In the case of the bis(dithiooxalato)nickelate(II), such a situation arises when RE = erbium.

Thus the CN change is likely to be due to steric effects. Our observation agrees with the data of Grenthe [9], who observed a modification of CN from 9 to 8 in the case of glycolato complexes: the CN is 9 from La to Gd and 8 from Gd to Lu. Steric effects are also probably responsible from the fact that the difference of bonds lengths Eu–O, Yb–O is higher than the difference of radius between the two RE.

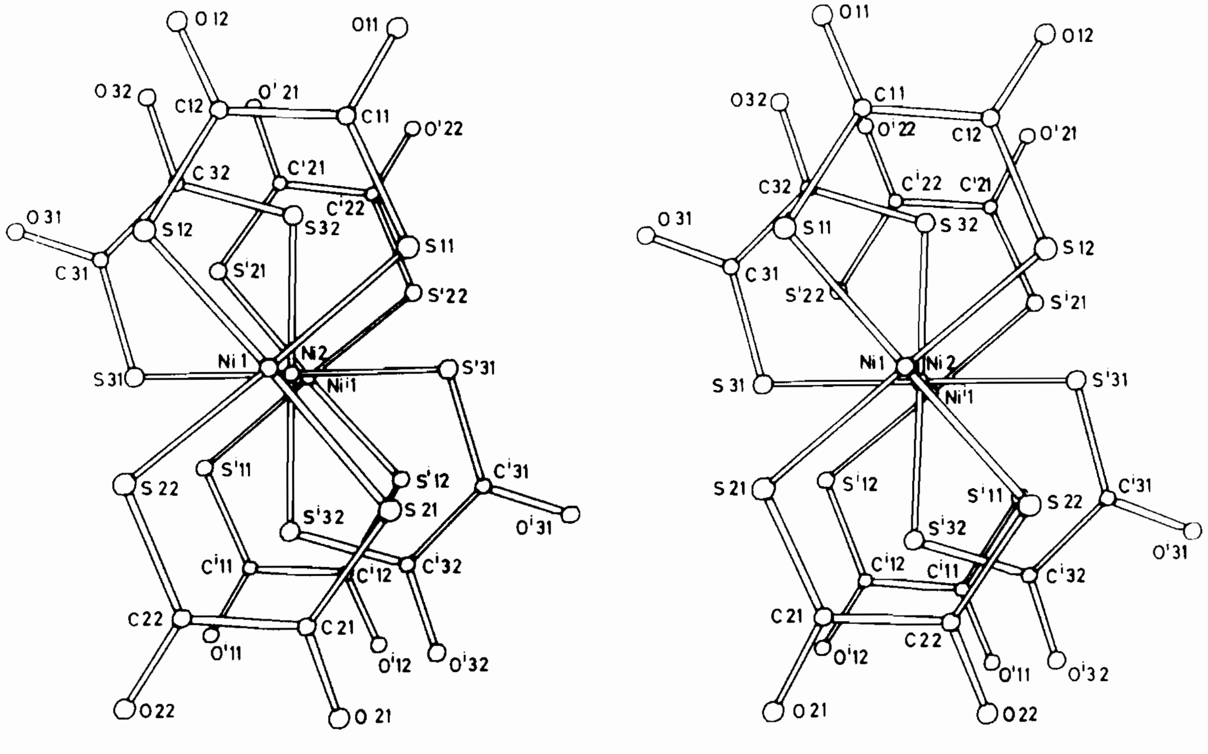

IIIa

IIIb

Fig. 3. Ortep drawing of stacking anions $Ni(S_2C_2O_2)^{2-}$ in: IIIa: the monoclinic structure; IIIb: the triclinic structure.

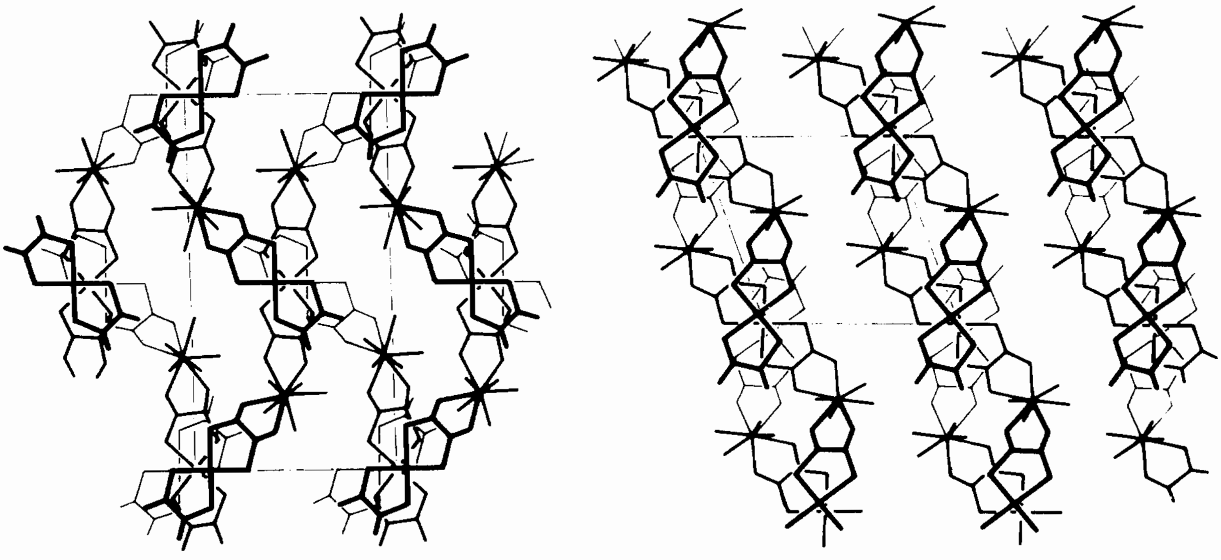

IVa

IVb

Fig. 4. View of the structures of $(RE)_2(H_2O)_{2n}Ni_3(S_2C_2O_2)_6, xH_2O$ down to the *a* axis. The intercalated water molecules are not represented. IVa: monoclinic structure; IVb: triclinic structure.

TABLE VI. Selected Interatomic Distances (Å).

Europium compound		Ytterbium compound	
O_{21}–O_{22}	2.615(7)	O_{21}–O_{22}	2.599(5)
O_{21}–Ow(1)	2.913(2)		
O_{21}–Ow(3)	2.949(7)		
O_{21}–O_{31}	2.986(4)		
O_{32}–O_{31}	2.638(7)	O_{32}–O_{31}	2.600(4)
O_{32}–Ow(2)	2.741(7)	O_{32}–Ow(2)	2.875(6)
O_{32}–Ow(3)	2.843(4)	O_{32}–Ow(3)	2.861(6)
O_{32}–Ow(4)	2.888(7)		
Ow(5)–O_{22}	2.747(9)	Ow(4)–Ow(5)	2.694(7)
Ow(5)–Ow(2)	2.783(8)	Ow(4)–Ow(3)	2.765(6)
Ow(5)–Ow(4)	2.894(9)	Ow(4)–O_{31}	2.834(6)
Ow(5)–Ow(1)	2.900(9)	Ow(4)–O_{21}	3.190(6)

The loss of one water molecule between the two structures involves a rearrangement of the coordination polyhedron of the RE: a rocking of the ligand bite O_{21}–O_{22} takes place, the two oxygen atoms becoming located on a basis of the trigonal prism while a water molecule is shifted from the basis of the trigonal prism towards a capping position (Fig. 2). A hypothesis can be formulated to account for this rearrangement.

In their study about eight coordination Burdett *et al.* [10] noticed that systems having the d^0 electronic configuration of the type ML_8 favour particularly the bicapped trigonal prism structure. Moreover, they indicated that the energy minima for the ideal bicapped trigonal prism corresponds, for the d^0 configuration, to an angle of 120° between the capping ligands (O_{32}YbOw(4) in Fig. 2).

The observed angles O_{21}–RE–O_{22} and O_{31}–RE–O_{32} are 62°66 and 63°47 for the monoclinic structure, while they become respectively 67°33 and 66°30 for the triclinic structure. The distances O_{21}–O_{22} and O_{31}–O_{32} are 2.615 Å and 2.638 Å for the europium compound and 2.599 Å, 2.600 Å for the ytterbium compound. These angles and distances must satisfy the constraints imposed by the geometry of both the dithiooxalate group and the rare-earth environment. In the bicapped trigonal prism (Fig. 2) the observed angle between the capping positions O_{32}–Yb–Ow(4) is 128°19, a value which is not very far from that corresponding to a maximal stabilization of this configuration. The water molecule Ow(4) is in close contact with the water molecules Ow(3) and Ow(1) (Table IV), and it is likely that these contacts participate to the polyhedron stabilization.

Let us suppose that there is no rocking of the ligand O_{21}–O_{22} between the two structures, when the tricapped trigonal prism is transformed into a bicapped trigonal prism. Under these conditions the angle O_{21}–Yb–O_{22} would be the one observed for Ow(4)–Yb–O_{21}, *i.e.* 85°83; such an angle appears somewhat different from that observed, and is probably incompatible with the geometry of the dithiooxalate group. So if we assume that it is not possible to lessen this angle without modifying the parameters responsible for the stabilization of the polyhedron, the rearrangement of the ligand O_{21}–O_{22} and of the water molecule becomes conceivable. Such a rearrangement does not modify the conformation of the hpe, and particularly the angles Ni(1)–RE–Ni(2) are very similar in both structures.

Conclusion

The family of hydrated bis(dithiooxalato)nickelate(II) rare-earths has not up to now presented any physical unusual properties. New series of rare-earths complexes of dithiooxalates have been synthesized by substituting Cu, Pd or Pt to Ni. The study of these compounds is now in progress.

References

1 A. Gleizes, F. Maury and J. Galy, *Inorg. Chim. Acta, 41*, 185 (1980).
2 F. Maury, A. Gleizes and J. Galy, *C.R. Acad. Sci. Paris, 291C*, 49 (1980).
3 A. Gleizes and M. Verdaguer, *J. Am. Chem. Soc., 1103*, 7373 (1981).
4 J. C. Trombe, A. Gleizes and J. Galy, *C.R. Acad. Sci. Paris, 294C*, 1369 (1982).
5 J. Flahaut, 'Les éléments des Terres-Rares', Masson, Paris (1969).
6 D. T. Cromer and J. T. Waber, 'International Tables for X-ray Crystallography', vol. IV, Table 2.2.A, Kynoch Press, Birmingham (1974).
7 A. Gleizes, F. Maury, P. Cassoux and J. Galy, *Z. Krist., 155*, 293 (1981).
8 L. Pauling, 'The Nature of the Chemical Bond', 3rd Ed., New York, Cornnel, University Press, Ithaca (1960).
9 E. Grenthe, Coll. Int. CNRS 'Les Eléments des Terres Rares', CNRS éditeur, Paris 1970, no. 180, 309–317.
10 J. K. Burdett, R. Hoffmann and R. C. Fay, *Inorg. Chem., 17*(9), 2553 (1978).